

Supporting information

Machine learning-based comprehensive survey on lithium-rich cathode materials

Akihisa TSUCHIMOTO, Masashi OKUBO, and Atsuo YAMADA *

Department of Chemical System Engineering, School of Engineering, The University of Tokyo,

Hongo 7-3-1, Bunkyo-ku, Tokyo 113-8656, Japan

* ayamada@g.ecc.u-tokyo.ac.jp

Conditions	Excess Li	Co/M ratio	Electrode weight /mg	Cutoff voltage (upper) /V	C rate /mAh g ⁻¹
Maximum	0.3	0.39	5.0	4.8	250
Minimum	0.1	0.0	1.5	4.5	10

Table S1. The range of each condition. Excess Li corresponds to x in $\text{Li}_{1+x}\text{M}_{1-x}\text{O}_2$. Co ratio is calculated by the following equation: $\text{Co ratio} = N_{\text{Co}} / (N_{\text{Co}} + N_{\text{Ni}} + N_{\text{Mn}})$. (N_M is molar number of contained each transition metal.)

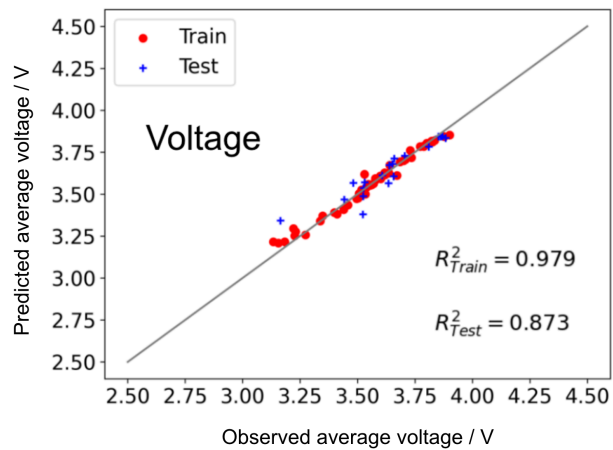
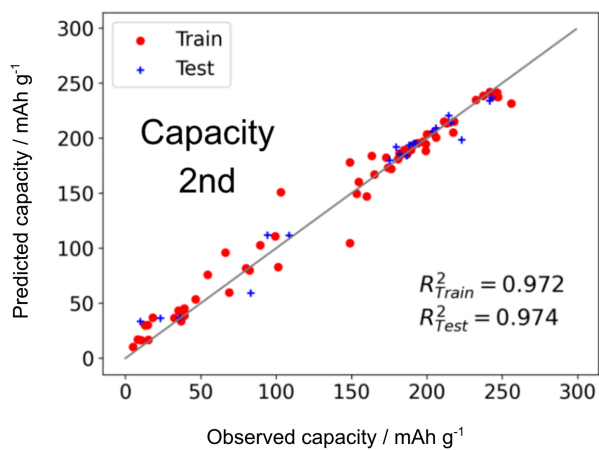


Figure S1. Comparison of observed and predicted capacity and average voltage of $\text{Li}_{1+x}[\text{Ni}, \text{Mn}, \text{Co}]_{1-x}\text{O}_2$ in the 2nd cycle.

Coulombic efficiency in the 2nd cycle

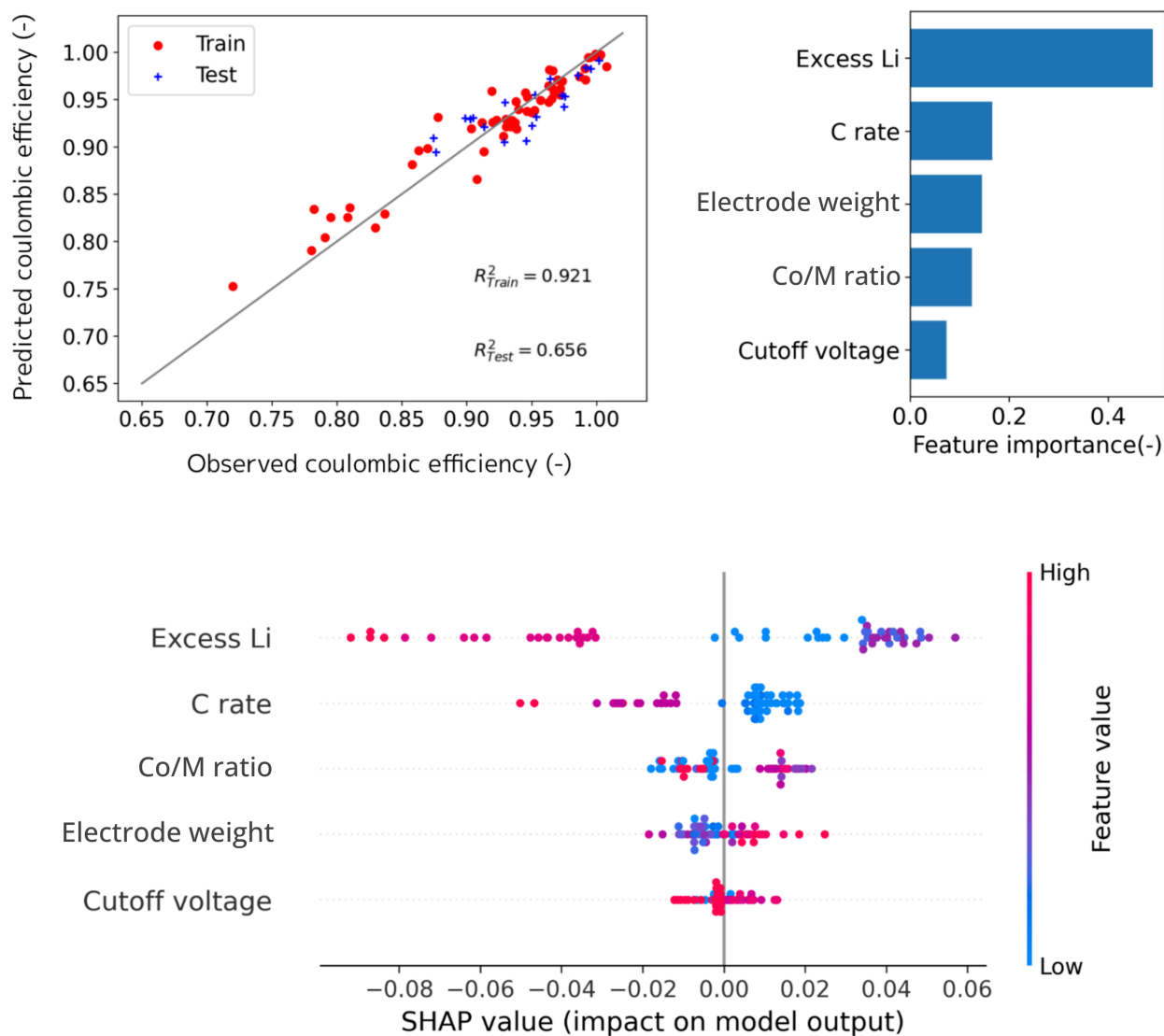


Figure S2. (a) Diagnostic plots and (b) feature importance of the prediction model for coulombic efficiency of $\text{Li}_{1+x}[\text{Ni}, \text{Mn}, \text{Co}]_{1-x}\text{O}_2$ in the 2nd cycle. (c) SHAP values of each feature in this prediction model.

Voltage hysteresis in the 2nd cycle

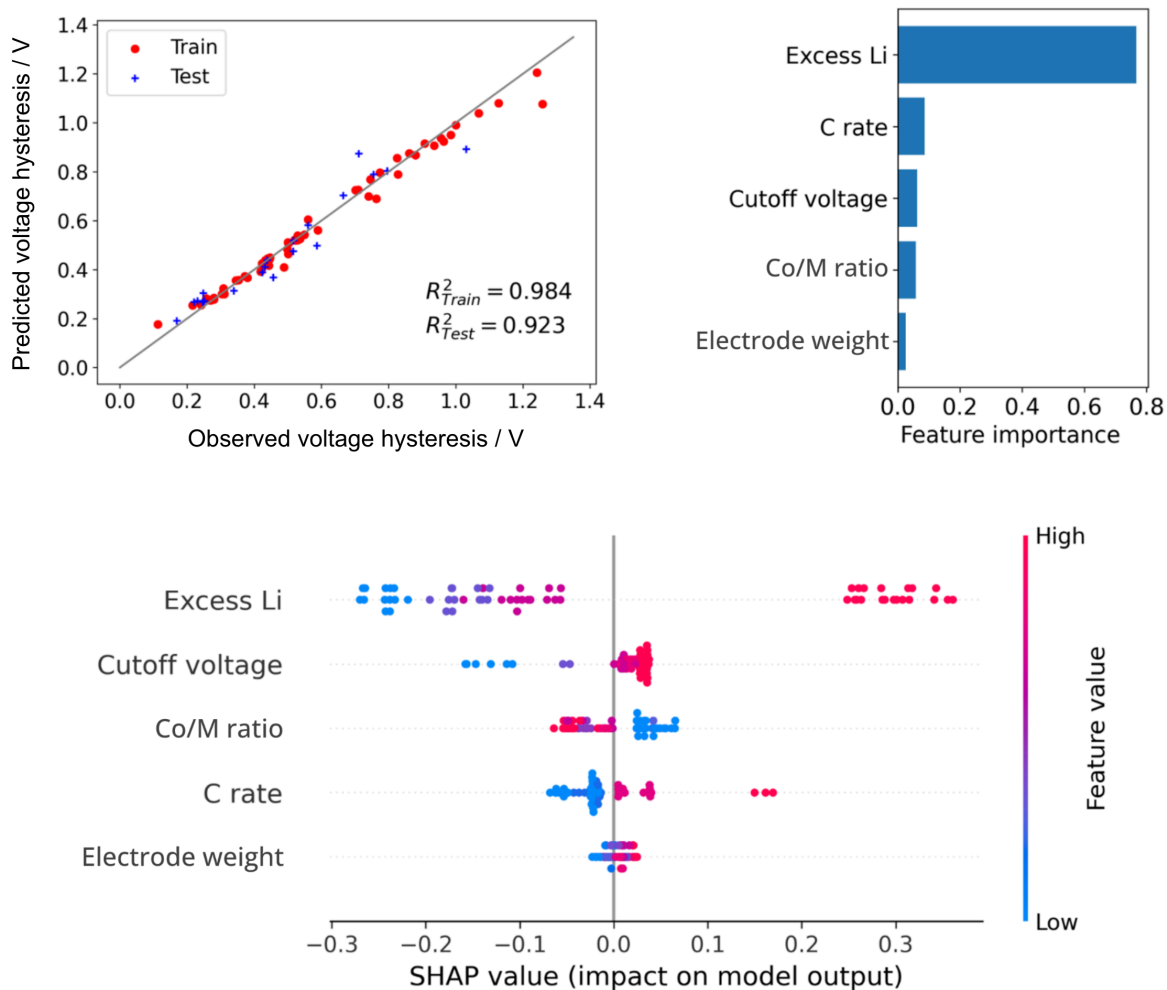


Figure S3. (a) Diagnostic plots and (b) feature importance of the prediction model for voltage hysteresis of $\text{Li}_{1+x}[\text{Ni}, \text{Mn}, \text{Co}]_{1-x}\text{O}_2$ in the 2nd cycle. (c) SHAP values of each feature in this prediction model.

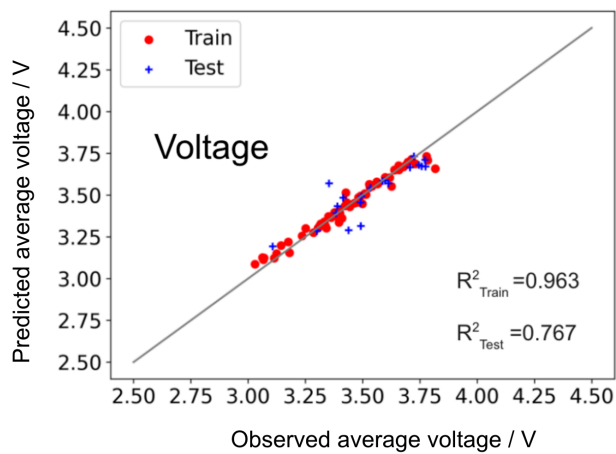
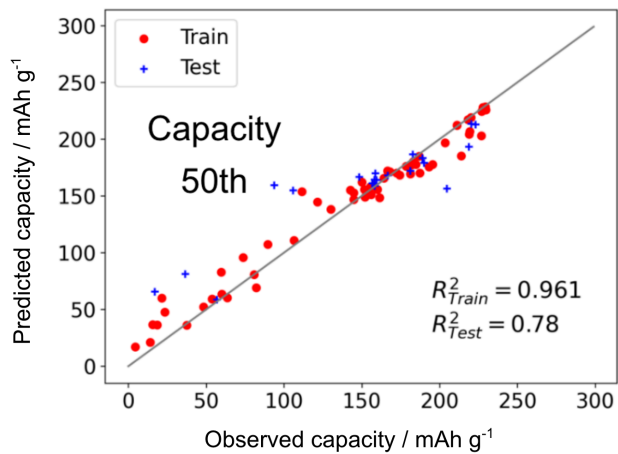


Figure S4. Comparison of observed and predicted capacity and average voltage of $\text{Li}_{1+x}[\text{Ni}, \text{Mn}, \text{Co}]_{1-x}\text{O}_2$ in the 2nd cycle.

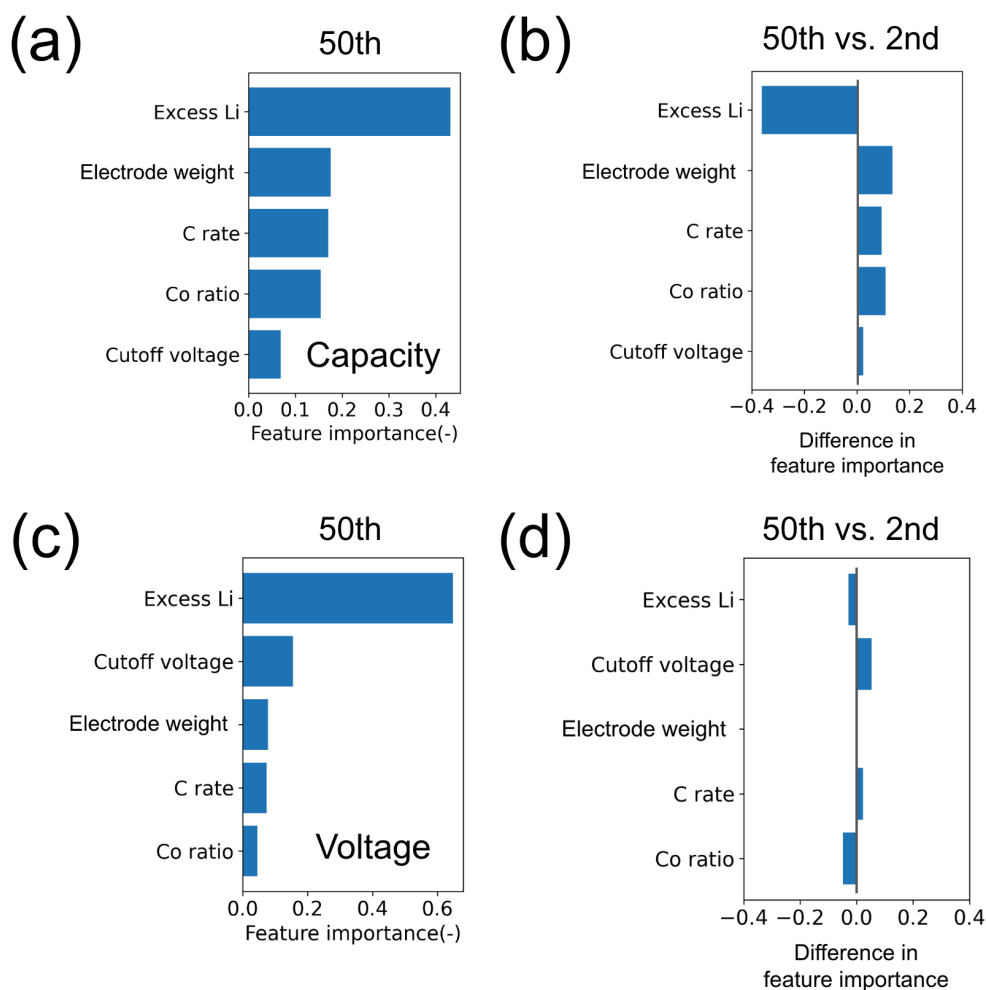


Figure S5. Feature importance in the prediction model for (a) capacity and (b) voltage at the 50th cycle and (c) (d) the change in feature importance comparing the 50th cycle with the 2nd cycle.

As for the weight of electrode, one possible explanation is that the higher concentration of slurry causes lower porosity of the electrodes, leading to suppression of degradation^{1,2}.

Voltage hysteresis in the 50th cycle

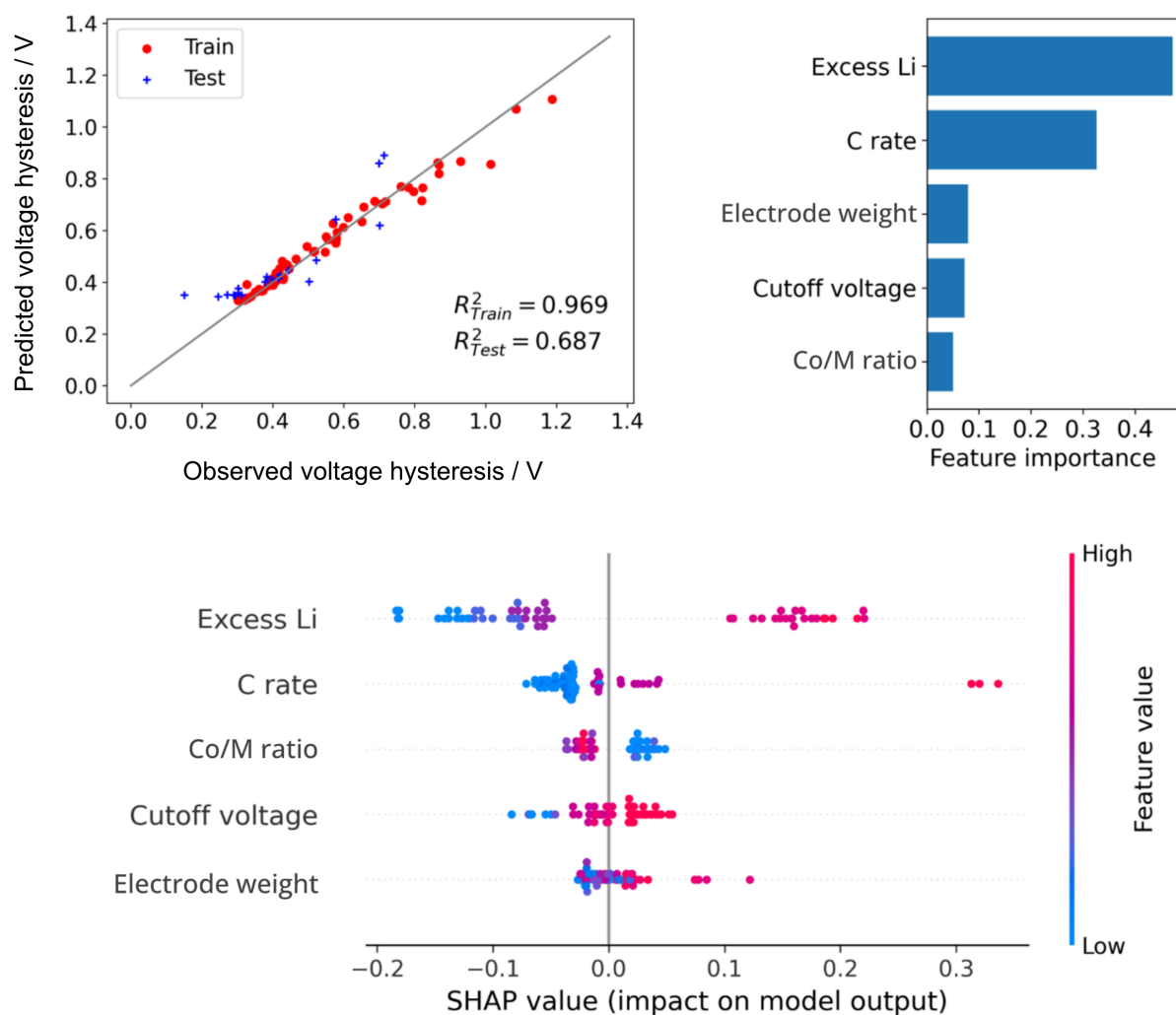


Figure S6. (a) Diagnostic plots and (b) feature importance of the prediction model for voltage hysteresis of $\text{Li}_{1+x}[\text{Ni}, \text{Mn}, \text{Co}]_{1-x}\text{O}_2$ in the 50th cycle. (c) SHAP values of each feature in this prediction model.

Presumably, the voltage hysteresis becomes larger under the higher C rates because the electrode-electrolyte interfacial resistance increases with repeating charge/discharge cycles.

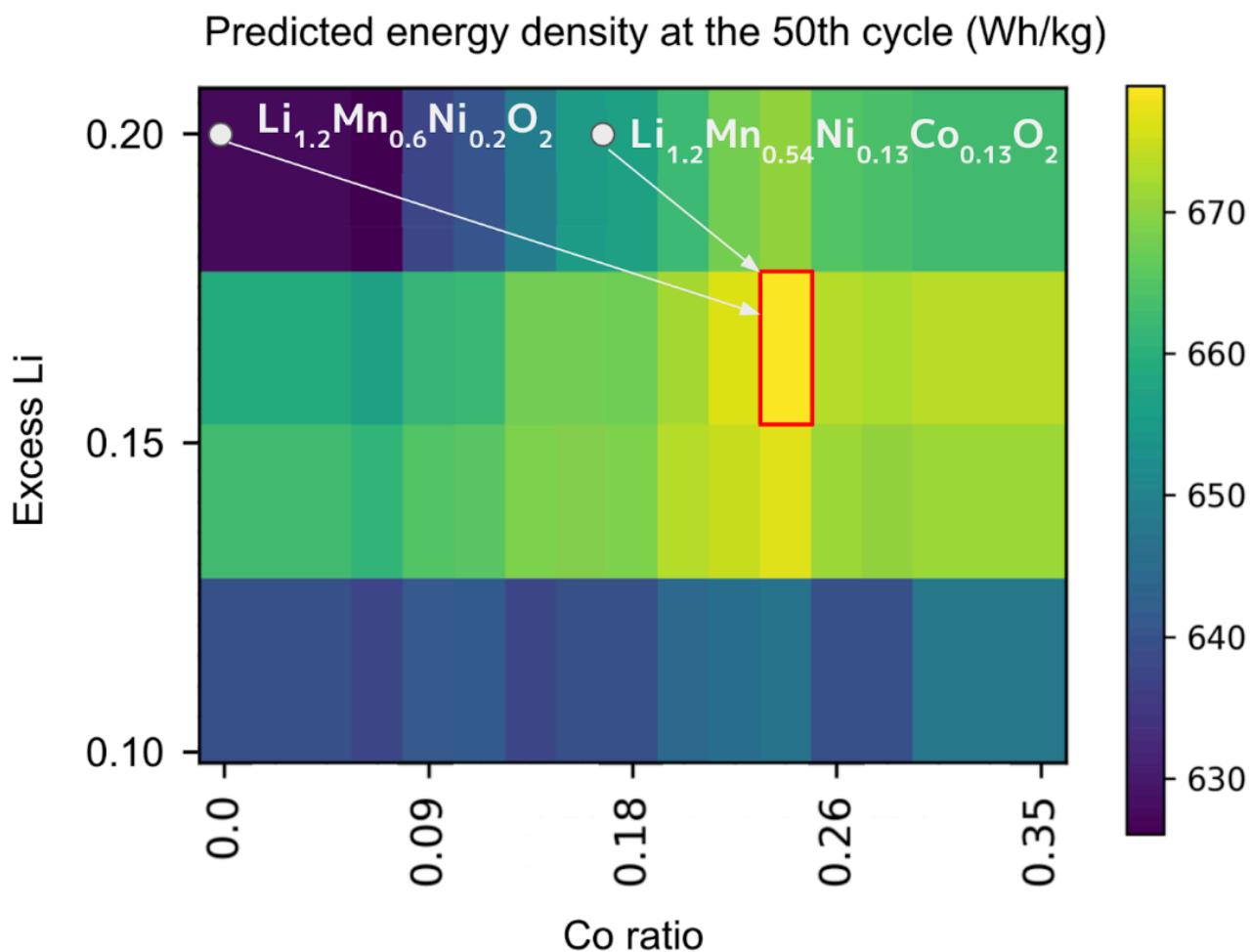


Figure S7. Optimized Li-rich cathodes composition for long-term cycle. The predicted energy density of Li-rich cathode materials at the 50th cycle when C rate, cutoff voltage and electrode weight are fixed to 20 mA/g, 4.8 V and 3 mg, respectively. $\text{Li}_{1.16}\text{Ni}_{0.14}\text{Mn}_{0.49}\text{Co}_{0.20}\text{O}_2$ shows the highest energy density. Note that fine tuning of conditions is not within the scope of this study.

1. Yu, S., Kim, S., Kim, T. Y., Nam, J. H. & Cho, W. I. Model Prediction and Experiments for the Electrode Design Optimization of LiFePO₄/Graphite Electrodes in High Capacity Lithium-ion Batteries. *Bull. Korean Chem. Soc.* **34**, 79–88 (2013).
2. Gallagher, K. G., Trask, S. E., Bauer, C., Woehrle, T., Lux, S. F., Tschech, M., Lamp, P., Polzin, B. J., Ha, S., Long, B., Wu, Q., Lu, W., Dees, D. W. & Jansen, A. N. Optimizing Areal Capacities through Understanding the Limitations of Lithium-Ion Electrodes. *J. Electrochem. Soc.* **163**, A138 (2015).